Selective area growth and characterization of GaN nanocolumns, with and without an InGaN insertion, on semi-polar (11–22) GaN templates

A. Bengoechea-Encabo, S. Albert, J. Zuñiga-Perez, P. de Mierry, A. Trampert, F. Barbagini, M. A. Sanchez-Garcia, and E. Calleja

Citation: Applied Physics Letters **103**, 241905 (2013); doi: 10.1063/1.4846455
View online: http://dx.doi.org/10.1063/1.4846455
View Table of Contents: http://scitation.aip.org/content/aip/journal/apl/103/24?ver=pdfcov
Published by the AIP Publishing

Selective area growth and characterization of GaN nanocolumns, with and without an InGaN insertion, on semi-polar (11–22) GaN templates

A. Bengoechea-Encabo,[1,a)] S. Albert,[1,a)] J. Zuñiga-Perez,[2] P. de Mierry,[2] A. Trampert,[3] F. Barbagini,[1] M. A. Sanchez-Garcia,[1] and E. Calleja[1]
[1]*ISOM and Departamento de Ingenieria Electronica, ETSI Telecomunicacion, Universidad Politecnica de Madrid, Ciudad Universitaria s/n 28040 Madrid, Spain*
[2]*CRHEA-CNRS, 06560 Valbonne, France*
[3]*Paul-Drude-Institut für Festkörperelektronik, Hausvogteiplatz 5-7, 10117 Berlin, Germany*

(Received 26 July 2013; accepted 26 November 2013; published online 10 December 2013)

The aim of this work is the selective area growth (SAG) of GaN nanocolumns, with and without an InGaN insertion, by molecular beam epitaxyon semi-polar (11–22) GaN templates. The high density of stacking faults present in the template is strongly reduced after SAG. A dominant sharp photoluminescence emission at 3.473 eV points to high quality strain-free material. When embedding an InGaN insertion into the ordered GaN nanostructures, very homogeneous optical properties are observed, with two emissions originating from different regions of each nanostructure, most likely related to different In contents on different crystallographic planes. © *2013 AIP Publishing LLC*. [http://dx.doi.org/10.1063/1.4846455]

III-nitrides have been extensively studied during the last years in order to fabricate optoelectronic devices due to their unique properties such as the tunability of their optical bandgap, covering a wide spectrum from the IR to the UV, as well as a high thermal and chemical stability. Most of these works focused on III-nitrides grown along the polar [0001] direction, with emphasis on developing commercial InGaN-based Light Emitting Diodes (LED) and Laser Diodes (LD). However, the internal polarization fields (spontaneous and/or piezoelectric) are very strong in heterostructures grown along this polar direction. The associated Quantum Confined Stark Effect affects detrimentally the internal quantum efficiency, and causes a blue shift of the electroluminescence peak with increasing current, due to screening of the internal electric field. In order to reduce or even avoid this internal polarization field, growth on semi-polar and non-polar crystal orientations has been suggested and demonstrated.[1,2] Up to now, the best results have been obtained when growing on nonpolar or semipolar bulk substrates[3] but due to limitations of bulk GaN substrates (in terms of size and price), heteroepitaxy on *r*-plane and *m*-plane sapphire has been the most common approach. This heteroepitaxial growth results typically in GaN templates with large density of stacking faults ($>10^5\,cm^{-1}$) and of their associated partial dislocations.[4]

Different strategies are used in order to increase the material quality.[5] As in the case of polar GaN, the epitaxial lateral overgrowth (ELO) technique has been implemented in metal organic chemical vapor deposition (MOCVD) to grow semi-polar (11–22) GaN layers with reduced defects density.[6,7] An alternative approach is the use of selective area growth (SAG) by molecular beam epitaxy (MBE), which already demonstrated the growth of high quality (In)GaN nanocolumns (NC) on *c*-plane GaN/sapphire templates,[8–11] as well as on nonpolar *a*-plane GaN templates.[12]

This work presents results on SAG of GaN nanostructures, grown by plasma-assisted MBE (PA-MBE), with and without an insertion of InGaN, on semi-polar (11–22) GaN templates. It will be shown that due to SAG, most of the basal stacking faults (BSFs) present in the initial GaN template are filtered, drastically improving the optical quality of the nanostructures. Furthermore, when embedding an InGaN insertion into the nanostructures, the In incorporation is shown to strongly depend on the crystallographic orientation, being significantly larger at the apex of the nanostructures (polar and semi-polar facets) than on the lateral non-polar facets.

The samples were grown in a Riber Compact 21 PA-MBE system, with an rf-plasma source for active nitrogen, and standard Knudsen cells for Ga and In. Molecular fluxes were calibrated in (0001) GaN and InN layers and are given in growth rate units (nm/min).[13] Substrates were (11–22) GaN templates grown by MOCVD on *m*-plane sapphire.

Prior to the growth, Ti nanohole masks were fabricated on (11–22) GaN templates by colloidal lithography.[12] Nanoholes were arranged in a compact hexagonal lattice with an average pitch of 270 nm and diameters of 200 nm. The resulting nanohole density was around $1.6 \times 10^9\,cm^{-2}$. The growth of the GaN NCs was performed with a Ga-flux of $\Phi_{Ga} = 18.5$ nm/min and a nitrogen flux of $\Phi_N = 5$ nm/min at 880 °C (thermocouple) for 3 h. Then, an InGaN insertion was grown at 625 °C (thermocouple), with $\Phi_{Ga} = 4.3$ nm/min, $\Phi_{In} = 4.3$ nm/min, and $\Phi_N = 14$ nm/min, during 160 s. The InGaN insertion was capped with a GaN layer grown for 5 min, at the same temperature (625 °C) and with $\Phi_{Ga} = 4.3$ nm/min and $\Phi_N = 14$ nm/min (just closing the In shutter). Samples were characterized by scanning (SEM) and transmission electron microscopy (TEM), photoluminescence (PL) excited by a He-Cd laser ($1\,W/cm^2$), and cathode-luminescence (CL).

Figures 1(a) and 1(b) show SEM images (top and bird's-eye views, respectively) of the GaN SAG nanostructures. The images show nanostructures tilted around 32° relative to the substrate surface.

[a)]A. Bengoechea-Encabo and S. Albert contributed equally to this work.

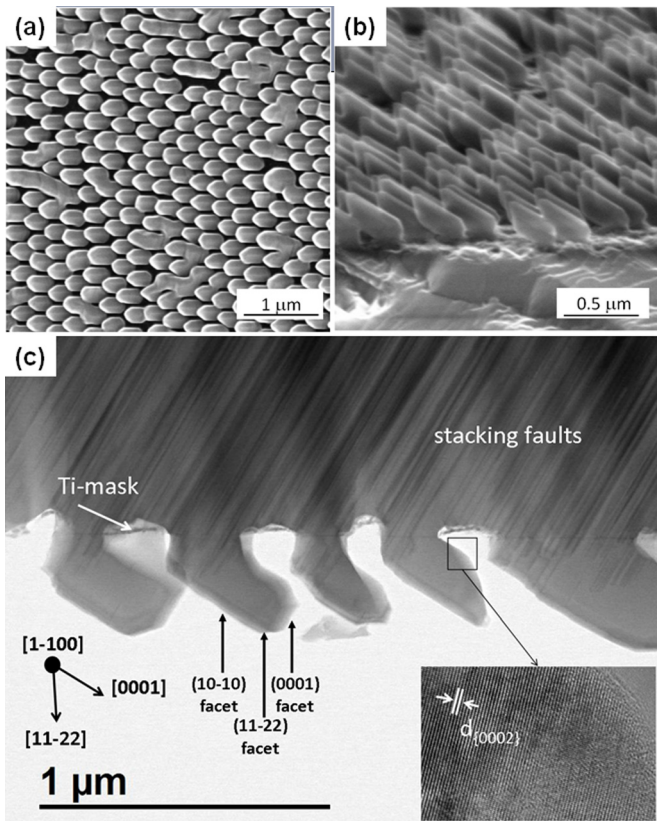

FIG. 1. SEM images of the ordered GaN NCs on a semi-polar (11–22) GaN template: top- (a) and bird's-eye (b) views. In (c), TEM image showing the tilted NCs with the long axis being parallel to the Ga-polar [0001] and the filtering effect of the stacking faults from the template. The three facets exposed to the molecular beams are indicated in the figure.

TEM images (Figure 1(c)) prove the GaN nanostructures elongation (preferential growth axis) parallel to the [0001] Ga-polar direction and the perfect alignment with the substrate. Two features are noteworthy: On the one hand, three facets different in nature (polar, semipolar, and nonpolar) are exposed to the molecular beams; on the other hand, most of the GaN nanostructures volume seems to be free of defects, because stacking faults only reach the lower part of them.

The improvement in optical quality is further confirmed by low temperature (8 K) PL measurements (Figure 2). Indeed, the broad emission from the (11–22) GaN template, at around 3.43 eV, is due to luminescence from BSFs.[14] After SAG, an enhanced band edge emission related to the donor bound exciton D^0X at 3.473 eV, nondistinguishable before, with a line width of only 2.7 meV, becomes dominant. This indicates a high quality and strain-free material. In addition, a weak emission at 3.42 eV (due to BSFs) can be still observed, which is assumed to originate from either the underlying GaN template or from the bottom of the NCs (Figure 1(c)).

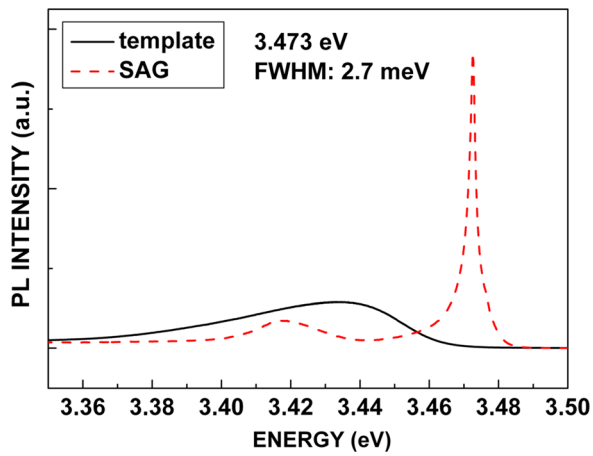

FIG. 2. Low temperature (8 K) PL spectra of the bare (11–22) GaN template and after SAG of GaN NCs.

In a second step, an InGaN insertion was embedded into the GaN nanostructures and capped by GaN, as explained in the experimental section.

Figures 3(a) and 3(b) show SEM images (top and bird's-eye views, respectively) of the GaN/InGaN/GaN SAG nanostructures. The images show nanostructures with a morphology that is rather similar to the one observed for GaN structures shown in Figures 1(a) and 1(b). As shown in Figure 3(e), room temperature (RT) CL spectra from the nanostructures ensemble (more than 2200 nanostructures in an area of

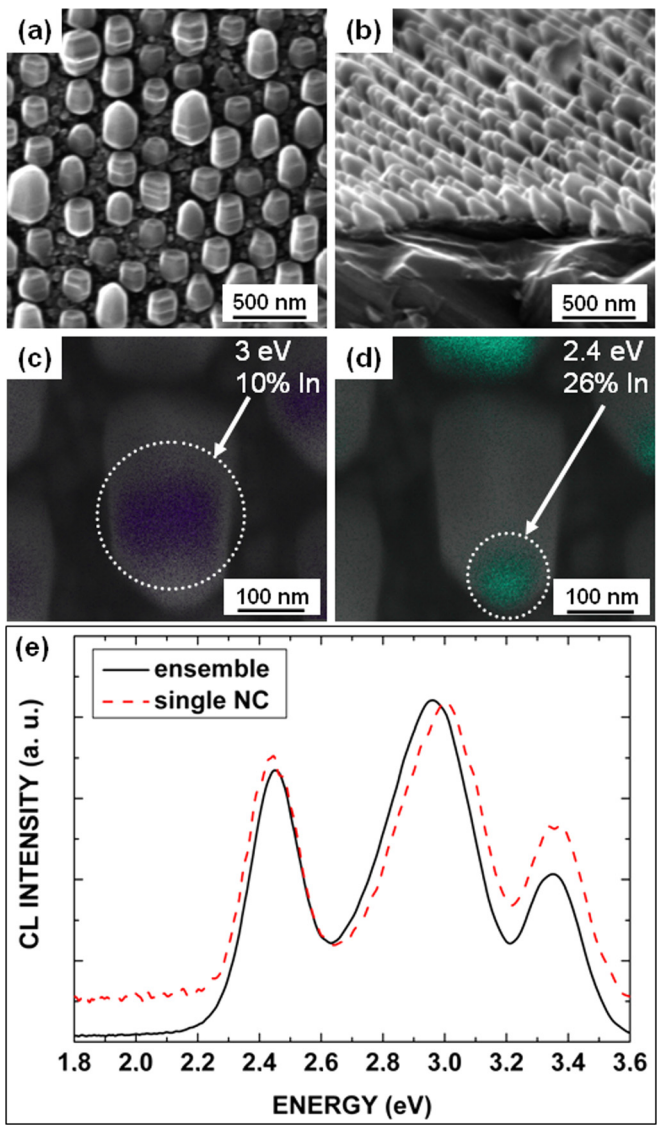

FIG. 3. SEM pictures of InGaN/GaN nanostructures in top view (a), and bird view (b). Spatially resolved InGaN-related emissions are shown in the SEM-CL measurements in (c) and (d). In (e), comparison of RT-CL spectra of a single InGaN/GaN nanostructure and an ensemble of around 2000 InGaN/GaN nanostructures.

about 15×13 μm^2) and from a single nanostructure, are almost identical. This homogeneity is one of the big advantages of the SAG. The RT-CL spectra in Figure 3(e) consist of three emission peaks, two of them related to InGaN, at 2.43 eV and 3 eV, respectively, and a third one due to GaN (~3.4 eV). Spatially resolved CL images (Figures 3(c) and 3(d)) show that the peak at 2.43 eV originates from the nanostructure apex, while the peak at 3 eV comes from a larger area below the apex. Assuming strain-free material, those emissions would correspond to $In_xGa_{1-x}N$ with x equal to 26% and 10%, respectively.[15]

According to the morphology of the GaN and InGaN/GaN nanostructures determined by TEM (Figure 1(c)) and SEM (Figures 3(a) and 3(b)) it can be assumed that the InGaN region with lower In content (3 eV peak emission) is grown on nonpolar planes, while the higher In content InGaN (2.43 eV) is grown on polar planes. Regarding the In incorporation on semipolar planes, which have been observed as well (Figure 1(c)), no clear statement can be made. It has been shown for PA-MBE, that In incorporates easier on (0001) polar planes than on (11–22) semi-polar planes,[16,17] but no experimental references regarding a difference in In incorporation on semi- and nonpolar planes could be found for the particular case of PA-MBE, although first-principle calculations indicate that In incorporation on (11–22) planes is higher than on nonpolar (10-10) planes.[18] It has to be noted that a different In incorporation depending on the crystalline plane has been reported for other growth techniques, like MOVPE[19,20] or ammonia MBE.[21]

In summary, ordered GaN/InGaN/GaN nanostructures were grown by SAG MBE on semipolar (11–22) GaN templates. PL and TEM analyses show a strong improvement in crystal quality after SAG due to an efficient filtering of most BSFs coming from the template. After SAG, PL emission is dominated by a strong donor-bound exciton line at 3.473 eV with a full width half-maximum of 2.7 meV.

Due to the SAG mode, embedding an InGaN insertion into the previous GaN NCs yields a very homogeneous array of nanostructures that give the same optical signature (RT-CL) both for a single nanostructure and an ensemble. CL spectra show two InGaN-related emission peaks at 2.43 eV and 3 eV that relate to regions with different In content within each single NC: Higher In contents are associated to In incorporation at polar or semi-polar planes (at the NCs apex) while lower In contents are achieved at non-polar facets.

Authors would like to acknowledge Dr. Uwe Jahn for fruitful discussion on cathode-luminescence technique. The presented work was partial financial support by the EU FP7 Contract GECCO 280694-2, the EU ITN RAINBOW PITN-GA-2008-213238, and the Spanish projects CAM/P2009/ESP-1503 and MICINN MAT2011-26703.

[1]P. Waltereit, O. Brandt, A. Trampert, H. T. Grahn, J. Menniger, M. Ramsteiner, M. Reiche, and K. H. Ploog, Nature **406**, 865 (2000).
[2]R. M. Farrel, E. C. Young, F. Wu, S. P. DenBaars, and J. S. Speck, Semicond. Sci. Technol. **27**, 024001 (2012).
[3]Y. Yoshizumi, M. Adachi, Y. Enya, T. Kyono, S. Tokuyama, T. Sumitomo, K. Akita, T. Ikegami, M. Ueno, K. Katayama, and T. Nakamura, Appl. Phys. Express **2**, 092101 (2009).
[4]P. Vennégues, Semicond. Sci. Technol. **27**, 024004 (2012).
[5]F. Scholz, Semicond. Sci. Technol. **27**, 024002 (2012).
[6]N. Kriouche, P. Vennégues, M. Nemoz, G. Nataf, and P. de Mierry, J. Cryst. Growth **312**, 2625 (2010).
[7]B. Lacroix, M. P. Chauvat, P. Ruterana, G. Nataf, and P. de Mierry, Appl. Phys. Lett. **98**, 121916 (2011).
[8]H. Sekiguchi, K. Kishino, and A. Kikuchi, Appl. Phys. Express **1**, 124002 (2008).
[9]K. Kishino, H. Sekiguchi, and A. Kikuchi, J. Cryst. Growth **311**, 2063 (2009).
[10]A. Bengoechea-Encabo, F. Barbagini, S. Fernandez-Garrido, J. Grandal, J. Ristic, M. A. Sanchez-Garcia, E. Calleja, U. Jahn, E. Luna, and A. Trampert, J. Cryst. Growth **325**(1), 89 (2011).
[11]S. Albert, A. Bengoechea-Encabo, M. A. Sánchez-García, X. Kong, A. Trampert, and E. Calleja, Nanotechnology **24**, 175303 (2013).
[12]A. Bengoechea-Encabo, S. Albert, M. A. Sanchez-Garcia, L. L. López, S. Estradé, J. M. Rebled, F. Peiró, G. Nataf, P. de Mierry, J. Zuñiga-Perez, and E. Calleja, J. Cryst. Growth **353**(1), 1 (2012).
[13]B. Heying, R. Averbeck, L. F. Chen, E. Haus, H. Riechert, and J. S. Speck, J. Appl. Phys. **88**(4), 1855 (2000).
[14]R. Liu, A. Bell, F. A. Ponce, C. Q. Chen, J. W. Yang, and M. A. Khan, Appl. Phys. Lett. **86**, 021908 (2005).
[15]J. Wu and W. Walukiewicz, Superlattices Microstruct. **34**, 63 (2003).
[16]A. Das, S. Magalhaes, Y. Kotsar, P. K. Kandaswamy, B. Gayral, K. Lorenz, E. Alves, P. Ruterana, and E. Monroy, Appl. Phys. Lett. **96**, 181907 (2010).
[17]A. Das, G. P. Dimitrakopulos, Y. Kotsar, A. Lotsari, Th. Kehagias, Ph. Komninou, and E. Monroy, Appl. Phys. Lett. **98**, 201911 (2011).
[18]J. E. Northrup, Appl. Phys. Lett. **95**, 133107 (2009).
[19]P. de Mierry, T. Guehne, M. Nemoz, S. Chenot, E. Beraudo, and G. Nataf, Jpn. J. Appl. Phys., Part 1 **48**, 031002 (2009).
[20]T. Wernicke, L. Schade, C. Netzel, J. Rass, V. Hoffmann, S. Ploch, A. Knauer, M. Weyers, U. Schwarz, and M. Kneissl, Semicond. Sci. Technol. **27**, 024014 (2012).
[21]D. A. Browne, E. C. Young, J. R. Lang, C. A. Hurni, and J. S. Speck, J. Vac. Sci. Technol. A **30**, 041513 (2012).